Förster Resonance Energy Transfer and the Local Optical Density of States in Plasmonic Nanogaps

Abdullah O. Hamza[1,2,3], Francesco N. Viscomi[1,2], Jean-Sebastien G. Bouillard[1,2*] and Ali M. Adawi[1,2*]

[1]Department of Physics and Mathematics, University of Hull, Cottingham road, HU6 7RX, UK

[2]G. W. Gray Centre for Advanced Materials, University of Hull, Cottingham road, HU6 7RX, UK

[3]Department of Physics, College of Science, Salahaddin University-Erbil

* a.adawi@hull.ac.uk and j.bouillard@hull.ac.uk

Abstract:

Förster resonance energy transfer (FRET) is a fundamental phenomenon in photosynthesis and is of increasing importance for the development and enhancement of a wide range of optoelectronic devices including colour tuning LEDs and lasers, light harvesting, sensing systems, and quantum computing. Despite its importance, fundamental questions still remain unanswered on the FRET rate dependency on the local density of optical states (LDOS). In this work, we investigate this directly, theoretically and experimentally, using 30 nm plasmonic nanogaps formed between a silver nanoparticle and an extended silver film, in which the LDOS can be controlled using the size of the silver nanoparticle. Experimentally, Uranin-Rhodamine 6G donor-acceptor pairs coupled to such nanogaps yielded FRET rate enhancements of 3.6 times. This, combined with 5 times enhancement in the emission rate of the acceptor, resulted in an overall 14 times enhancement in the acceptor's emission intensity. By tuning the nanoparticle size, we also show that the FRET rate in those systems is linearly dependent on the LDOS, a result which is directly supported by our Finite Difference Time Domain (FDTD) calculations. Our results provide a simple but powerful method to control FRET rate via a direct LDOS modification.

Förster resonance energy transfer (FRET) is a near field dipole-dipole energy transfer from an excited donor to a nearby ground-state acceptor emitter[1,2]. Typically FRET arises on donor-acceptor length, and plays a pivotal part inside complex molecular assemblies[3], monitoring nanoscale dynamics of protein[4] and in the photosynthetic process of plants and bacteria[5,6]. Furthermore, FRET is rapidly becoming of increasing importance as a mean of enhancing the functionality and efficiency of a wide range of optoelectronic devices including colour tuning LEDs[7], lasers[8], light harvesting[9], sensing systems[10], optical networks[11], quantum computing[12] and quantum logic gates[13]. However, achieving these technological promises is greatly limited by the intrinsic short range nature of FRET , making strategies to increase both the range and rate of FRET a critical development for those key enabling technologies.

An excited donor can either decay directly to its ground state through spontaneous emission process[14–16] or non-radiatively transfer energy to a nearby acceptor through FRET process[14–17]. In a ground-breaking theory paper[17] Dung *et al* showed that the FRET rate depends on the total Green function between the donor and the acceptor, while the spontaneous emission rate depends only on the imaginary part of the Green function at the donor location, a quantity that is directly proportional to the local density of optical states (LDOS). Accordingly, both spontaneous emission rate and FRET rate are affected by the local electromagnetic fields[15]. Having said that, the exact dependency of the FRET rate on the LDOS is still an ongoing debate between physicists in this field.

Several electromagnetic environments have been used to modify the FRET rate and study its dependence on the LDOS. Experimental and theoretical works obtain contradictory results about the nature of the FRET rate dependency on LDOS. Reports based on dielectric optical resonators[18–21] find that the FRET rate is independent of the LDOS. Just recently, Wubs and Vos[22] showed theoretically that the FRET rate is independent of the LDOS at the donor frequency for any nanophotonic medium with weak dispersion and hardly depends on the frequency-integrated LDOS. By contrast, a linear relation between FRET rate and LDOS is reported based on systems consisting of either metallic films[23,24] a single plasmonic nanoparticle[25], coupled plasmonic dimer[26] or an array of plasmonic nanoparticles[27]. Gonzaga-Galeana and Zurita-Sánchez[15] numerically found that the FRET rate in the present of metallic nanoparticles has approximately linear relation with LDOS above a certain threshold for the emission rate. On the other hand Bidault *et al*[28] reported a 5-fold increase of FRET rate in plasmonic dimer nanoantennas with no direct correlation between FRET rate enhancement

and LDOS. Ren *et al*[29] theoretically investigated the dependency of the FRET rate from a donor to an acceptor on the LDOS when they are located in the hotspots of a collinear trimer system. Depending on the system conditions and the relative strength of the electric field at the donor location to the field strength at the acceptor location, FRET rate can be either dependent (linearly or even exponentially) or independent on the LDOS.

Another important figure of merit is the FRET efficiency, which is a measure of the likelihood of the excited donor to undergo Förster process and can be define as

(1)

where is the FRET rate, is the donor spontaneous emission decay rate and the quantity is known as normalised FRET rate. The works of Ghenuche *et al*[26] and Bidault *et al*[28] show that coupled plasmonic dimers deteriorate the Förster efficiency by a factor of 3. These results are in agreement with the theoretical work of Zurita-Sánchez and Mendez-Villanueva[30] who attributed the reduction in the Förster efficiency to the simultaneous increase in the donor decay rate in the presence of the dimer. However, Torres *et al*[2] achieved up to 50% (33% without a dimer) FRET efficiency through careful alignment of the donor dipole moment relative to the acceptor one, and Higgins *et al*[31] achieved up to 50% Förster efficiency using an array of plasmonic nanotstructures. On the other hand FRET efficiency based on dielectric optical resonators[18,32] range from ~40% -75%.

In spite of these important results, the focus remains mainly on the use of localised surface plasmons (LSP) of small particle to achieve plasmonic nanogaps. Recently plasmonic nanogaps based on the coupling between a metallic nanoparticle and a continuum metallic film have attracted much attention to modify the spontaneous emission process and thus the LDOS[33–35], study light matter interaction in the strong coupling regime[36], enhance hot electrons generation[37] and probing molecular orientation *via* single molecule SERS[38,39].

In this work, we investigate the FRET rate and the FRET efficiency from an ensemble of donor-acceptor molecules located in the centre of a 30 nm plasmonic nanogap consisting of a silver nanoparticle coupled to an extended silver film (see Figure 1). We have found that the FRET rate can be enhanced by a factor of 3.6 times while retaining the FRET efficiency compared to vacuum. Furthermore, our work shows that the FRET rate in this type of nanogaps is linearly dependent on the LDOS. These results are combined with 5 times enhancement in the emission rate of the acceptor and 14 times enhancement in its intensity as compared to structures without nanogaps.

First, we numerically investigated the FRET process in a plasmonic nanogap by treating the donor and the acceptor as classical electric point dipoles. In this framework, the power transferred from the donor to the acceptor can be written as[14]

(2)

where is the emission/absorption frequency of the donor/acceptor, is a unit vector in the direction of the acceptor's dipole moment , is the electric field of the donor at the location of the acceptor (, and is the acceptor polarizability and can be related to the acceptor's dipole moment as .

The total power emitted by the donor in the absence of the acceptor in inhomogeneous environment is[14]

(3)

where is the emission frequency of the donor, is the donor's dipole moment and is the electric field at the location of donor's dipole.

The normalised energy transferred from donor to acceptor can be related to the normalised energy transfer rate through the expression[14]

(4)

where is the transferred power from the donor to the acceptor, is the power emitted by the donor in the absence of the acceptor in free space, is the energy transfer rate and is the emission rate of the donor in the absence of the acceptor in free space.

(Equation (2)) and (Equation (3)) are obtained by numerically solving Maxwell equations using the finite difference time domain (FDTD) method[40]. The advantage of the FDTD approach over other methods[41,42] is that it can be applied to arbitrary complex inhomogeneous media[16,43].

The investigated plasmonic nanogaps (Figure 1) consist of a silver nanoparticle of diameter *D*, a nanogap of width 30 nm, and an extended silver film of 100 nm thickness. In order to explore the effect of the plasmonic nanogap on the FRET efficiency and FRET rate, in the FDTD simulations, *D* was varied from 0 to 300 nm, where " " corresponds to the same geometry without the nanoparticle which we label as "off nanogap". The donor molecule is represented by a classical dipole with an oscillating field in the z-direction located at (r_D, 0, 0). In all calculations we assumed the dipole moment of the acceptor to be in the z-direction,

parallel to the nanogap field[38]. Experimental data from Johnson and Christy were used to describe the dielectric function of silver[44]. The refractive index of the host environment inside the gap is set to 1.43 representing the inert organic host matrix, Poly(methacrylic acid) (PMA). In all calculations, we employed a grid spacing of 1 nm, and stretched coordinate perfect matching layer boundary conditions. Calculations were terminated when the fields had decayed below 10^{-5} of their original value.

To study the influence of our plasmonic nanogaps on the FRET rate, we first considered a 30 nm nanogap formed between a 200 nm diameter silver particle and an extended silver film. A typical distribution of the normalised energy transfer rate is presented in Figure 2a. Here the donor emission wavelength was fixed at , corresponding to the maximum emission of the Uranin laser dye (also known as Disodium Fluorescein), which was used in the experiments. It can be seen that the normalised energy transfer rate is mainly localised within the nanogap region. In these calculations the position of the donor is fixed at the centre of the nanogap (0, 0, 0) and the normalised energy transfer rate is calculated for the acceptor positioned in the x-z plane (Figure 1). For an acceptor with a dipole moment in the z-direction the power transferred from the donor to the acceptor is proportional to the square of the z-component of the donor field at the acceptor location (see Equation (2)). For a donor dipole located in the centre of the plasmonic nanogap, the maximum value of arises within the nanogap region[33–35] explaining why is mainly concentrated within the nanogap. Figure 2b displays the relation between and the donor emission wavelength λ_D for the acceptor positioned along the line with . It can be seen that our nanogap provides up to 80 times enhancements in in the visible range. This behaviour illustrates that coupled plasmonic nanogaps are fundamentally different from single plasmonic nanoparticles where the FRET rate is mainly enhanced close to the surface plasmon resonance wavelength[45,46]. This difference is attributed to the mode hybridisation between the silver nanoparticle plasmons and the delocalised surface plasmons of the extended silver film[34,47] leading wider wavelength range.

As we discussed earlier, the dependence of the FRET rate on the LDOS is a debatable subject. In what follows, we study the relation between the FRET rate and the LDOS in our nanogaps. From the Fermi Golden Rule, the spontaneous decay rate is directly proportional to the LDOS at the donor position () and by treating the donor as a classical electric point dipole, the enhancement in both the spontaneous decay rate and can be related to the donor emitted power through the relation[14]

(5)

where is the vacuum optical density of states, can be either calculated directly from equation (3) or through the integration of the Poynting vector over a closed surface containing the donor dipole in the presence of the nanogap

(6)

where is a unit vector normal to the closed surface and is the magnetic field.

We altered the LDOS at the donor position () in two ways:

(1) by changing the donor location, , within the nanogap along the -axis (and) while keeping the gap-width *d* and the particle size *D* constants,

(2) by varying the diameter of the plasmonic nanoparticle[34], *D*, while keeping the donor at .

In all cases, the normalised energy transfer rate was calculated for an acceptor dipole moment in the z direction and located 10 nm away from the donor.

Plotting the calculated results of as a function of therefore allows visualising the evolution of the normalised FRET rate with the LDOS. This was done for the two cases above, (1) and (2), in Figure 2c and Figure 2d respectively. From those results, it is clear that increases linearly with the LDOS with a gradient of 1.23 when changing the particle size and a gradient of 0.90 when changing the donor position within the nanogap. These results are in line with the experimental work of Ghenuche et al[26] and the theoretical work of Ren *et al*[29] for relativity large nanogaps.

The FRET process was then investigated experimentally in equivalent plasmonic nanogaps formed between a silver nanoparticle of diameter 0 nm (off nanogap), 100 nm or 200 nm and an extended 100 nm thick silver film separated by a 30 nm gap. The active layer consists of a 10 nm PMA (Poly(methacylic acid), Scientific Polymer Products Inc.) layer doped with the donor-acceptor pair (Uranin-Rhodamine 6G), in 5% and 0.25% concentrations by weight in ethanol. The 10 nm PMA film was achieved by spin coating a solution of PMA in ethanol at a speed of for seconds. The active layer was sandwiched between two inert spacing layers of cross-soluble Zeonex (Zeon Chemicals Europe Ltd) in toluene to obtain a well-defined emission zone. The 10 nm Zeonex film was deposited by spin coating a solution of Zeonex in toluene at a speed of for seconds. Bruker Dektak XT profilometer was used to measure the thickness of all the used polymer layers. To complete the nanogaps, silver nanoparticles

(nanoComposix) suspended in ethanol at concentration ~ were spin-coated onto the Zeonex surface at a speed of for seconds. The donor-acceptor pair was designed for large spectral overlap between the donor emission and acceptor absorption spectra (Figure 3b).

The LDOS within our experimental nanogap was tuned by changing the sliver nanoparticle diameter with values of 0, 100 nm and 200 nm. In the experiment, the CW and time-resolved fluorescence measurements were performed using a home-built optical microscope. The donor was excited with a 405 nm picosecond (40 ps pulse durations and 80 MHz repetition rate) laser diode to match the Uranin absorption spectrum but not the Rhodamine 6G (see Figure 3b). The excitation laser was focused on the sample using a 100x magnification Mitutoyo infinity corrected long working distance objective lens with numerical aperture NA =0.9 providing a diffraction limited spot size of 550 nm diameter. The same objective was used to collect the donor/acceptor emission, which was then directed toward an iHR320 Horiba spectrometer where it was dispersed using a 150 lines/mm grating onto either a ProEM Princeton Instruments camera for CW fluorescence measurements or a Becker and Hickl HPM-100 detector for fluorescence time-resolved measurements.

To investigate the energy transfer in our samples, we first recorded the emission spectra of the donor/acceptor after donor excitation using plasmonic nanogaps with top particle sizes of 0, 100 and 200 nm. For comparison, we recorded the emission spectra from three different control samples; i) donor-acceptor on glass substrate, ii) donor only/acceptor only in 30 nm plasmonic nanogap with the same top particle sizes (Figure 4a and 4b).

In all donor-acceptor samples we see a strong reduction in the donor emission intensity (Figure 4a) combined with a strong enhancement in the acceptor emission signal (Figures 4a and 4b) compared to the corresponding control samples, clearly illustrating FRET is taking place in our plasmonic nanogaps. The enhancement in the acceptor emission intensity in the presence of the donor is three times stronger than the emission enhancement in the emission intensity of the acceptor only control samples (see Figure 4b), clearly showing that the observed strong enhancement in the acceptor signal cannot be attributed only to the modification in the LDOS. In addition, the measured enhancements in acceptor emission decay rate in the presence of the donor are very close to the of the acceptor only (Figure 4c), clearly demonstrating that the enhancements in the acceptor emission intensity in the presence of the donor are due to FRET.

In order to conclusively confirm FRET in the plasmonic nanogaps, and to determine its dependence on the LDOS, the fluorescence lifetime of the donor with and without the acceptor has been investigated (Figures 5a and 5b). The control samples with donor only allow to measure the LDOS as a function of the nanoparticle size, while the samples with the donor-acceptor pair allow to study the FRET rate as a function of the LDOS. In Figure 5a, we plot the emission intensity decay traces measured from the donor only samples coupled to plasmonic nanogaps with particles of diameter 0, 100, and 200 nm, together with a reference sample consisting of the polymer layers on glass. The comparison of emission decay rate for the donor only samples are summarised in Figure 5c and reveals clearly the possibility to control the LDOS by changing the particle size of the nanogap as we previously demonstrated theoretically[34]. The presence of the acceptor increases the donor emission decay rate further (see Figure 5b and 5c), clearly demonstrating the occurrence of FRET in our samples.

To quantify the FRET rate, , we write the total decay rate of the donor in the presence of the acceptor as , where accounts for the spontaneous decay rate and account for the FRET rate. This expression allows us to investigate the influence of the photonic environment surrounding the donor on the FRET rate . The results of this analysis are summarised in Figure 5c where the enhancement in due to the presence of the nanogap is clearly visible compared to the glass reference sample. Enhancement factors of 2 and 3.6 were obtained using a nanogap of particle size 100 nm and 200 nm respectively, demonstrating that can be modified using plasmonic nanogaps.

To evaluate the efficiency of FRET process in our samples, we calculated the Förster efficiency using the expression , and found a maximum efficiency of 0.43 using 200 nm particle size nanogaps (Figure 6a). These results indicate clearly that, with the right nanogap design, it is possible to enhance simultaneously the energy transfer rate and the Förster efficiency. Additionally, using the standard expression for the Förster radius[14] , in conjunction with the Förster efficiency for the reference sample on glass (Figure 6a), the donor-acceptor distance was calculated to be 9.3 nm, justifying the choice of donor-acceptor separation in our simulations.

To explore the relation between the energy transfer rate and the LDOS, we plot in Figure 6b the measured against where is equivalent to experimentally measuring the LDOS. Our experimental data shows a linear relationship between the energy transfer rate and the LDOS

in an excellent agreement with our FDTD in Figure 2d. These results indicate that the term in Equation (3) is close to in Equation 2[29] in our nanogaps.

In summary, we have investigated theoretically and experimentally the FRET process in plasmonic nanogaps consisting of a silver nanoparticle coupled to an extended silver film. In particular, we determined the effect of the LDOS on the FRET rate and efficiency. Our FDTD modelling showed that the FRET rate is linearly dependent on the LDOS. Experimentally we fabricated a series of equivalent nanogaps and observed a linear dependency of the FRET process on the LDOS, in good agreement with our FDTD simulations. Our results provide a simple but powerful approach to engineer FRET rates, an approach that will help guiding the design of new types of optoelectronic and light harvesting systems.

Acknowledgment

We thank the Higher Committee for Education Development in Iraq-HCED for supporting AOH to study for a PhD at the University of Hull and we thank the University of Hull for the provision of a PhD scholarship for FNV. This work was partially supported by the UK EPSRC through Grant EP/L025078/1 and EU grant POSEIDON ID 861950. We thank Stuart Harris at Zeon Chemicals Europe Ltd for the gift of the Zeonex polymer.

References

(1) Förster, T. Zwischenmolekulare Energiewanderung Und Fluoreszenz. *Ann. Phys.* **1948**, *437* (1–2), 55–75. https://doi.org/10.1002/andp.19484370105.

(2) De Torres, J.; Mivelle, M.; Moparthi, S. B.; Rigneault, H.; Van Hulst, N. F.; García-Parajó, M. F.; Margeat, E.; Wenger, J. Plasmonic Nanoantennas Enable Forbidden Förster Dipole-Dipole Energy Transfer and Enhance the FRET Efficiency. *Nano Lett.* **2016**, *16* (10), 6222–6230. https://doi.org/10.1021/acs.nanolett.6b02470.

(3) Teunissen, A. J. P.; Pérez-Medina, C.; Meijerink, A.; Mulder, W. J. M. Investigating Supramolecular Systems Using Förster Resonance Energy Transfer. *Chem. Soc. Rev.* **2018**, *47* (18), 7027–7044. https://doi.org/10.1039/c8cs00278a.

(4) Selvin, P. R. The Renaissance of Fluorescence Resonance Energy Transfer. *Nat. Struct. Biol.* **2000**, *7* (9), 730–734. https://doi.org/10.1038/78948.

(5) Sekar, R. B.; Periasamy, A. Fluorescence Resonance Energy Transfer (FRET) Microscopy Imaging of Live Cell Protein Localizations. *J. Cell Biol.* **2003**, *160* (5), 629–633. https://doi.org/10.1083/jcb.200210140.

(6) Mirkovic, T.; Ostroumov, E. E.; Anna, J. M.; Van Grondelle, R.; Govindjee; Scholes,

G. D. Light Absorption and Energy Transfer in the Antenna Complexes of Photosynthetic Organisms. *Chem. Rev.* **2017**, *117* (2), 249–293. https://doi.org/10.1021/acs.chemrev.6b00002.

(7) Ghataora, S.; Smith, R. M.; Athanasiou, M.; Wang, T. Electrically Injected Hybrid Organic/Inorganic III-Nitride White Light-Emitting Diodes with Nonradiative Förster Resonance Energy Transfer. *ACS Photonics* **2018**, *5* (2), 642–647. https://doi.org/10.1021/acsphotonics.7b01291.

(8) Gartzia-Rivero, L.; Cerdán, L.; Bañuelos, J.; Enciso, E.; López Arbeloa, Í.; Costela, Á.; García-Moreno, I. Förster Resonance Energy Transfer and Laser Efficiency in Colloidal Suspensions of Dye-Doped Nanoparticles: Concentration Effects. *J. Phys. Chem. C* **2014**, *118* (24), 13107–13117. https://doi.org/10.1021/jp503218z.

(9) Wu, C.; Zheng, Y.; Szymanski, C.; McNeill, J. Energy Transfer in a Nanoscale Multichromophoric System: Fluorescent Dye-Doped Conjugated Polymer Nanoparticles. *J. Phys. Chem. C* **2008**, *112* (6), 1772–1781. https://doi.org/10.1021/jp074149+.

(10) Peng, H. S.; Stolwijk, J. A.; Sun, L. N.; Wegener, J.; Wolfbeis, O. S. A Nanogel for Ratiometric Fluorescent Sensing of Intracellular PH Values. *Angew. Chemie - Int. Ed.* **2010**, *49* (25), 4246–4249. https://doi.org/10.1002/anie.200906926.

(11) Mehlenbacher, R. D.; McDonough, T. J.; Grechko, M.; Wu, M. Y.; Arnold, M. S.; Zanni, M. T. Energy Transfer Pathways in Semiconducting Carbon Nanotubes Revealed Using Two-Dimensional White-Light Spectroscopy. *Nat. Commun.* **2015**, *6*, 1–7. https://doi.org/10.1038/ncomms7732.

(12) Lovett, B. W.; Reina, J. H.; Nazir, A.; Briggs, G. A. D. Optical Schemes for Quantum Computation in Quantum Dot Molecules. *Phys. Rev. B - Condens. Matter Mater. Phys.* **2003**, *68* (20), 1–18. https://doi.org/10.1103/PhysRevB.68.205319.

(13) Barenco, A.; Deutsch, D.; Ekert, A.; Jozsa, R. Conditional Quantum Dynamics and Logic Gates. *Phys. Rev. Lett.* **1995**, *74* (20), 4083–4086. https://doi.org/10.1103/PhysRevLett.74.4083.

(14) Novotny, L.; Hecht, B. *Principles of Nano-Optics*; Cambridge University Press: Cambridge, 2012. https://doi.org/10.1017/CBO9780511794193.

(15) Gonzaga-Galeana, J. A.; Zurita-Sánchez, J. R. A Revisitation of the Förster Energy Transfer near a Metallic Spherical Nanoparticle: (1) Efficiency Enhancement or Reduction? (2) the Control of the Förster Radius of the Unbounded Medium. (3) the Impact of the Local Density of States. *J. Chem. Phys.* **2013**, *139* (24). https://doi.org/10.1063/1.4847875.

(16) De Roque, P. M.; Hulst, N. F. V.; Sapienza, R. Nanophotonic Boost of Intermolecular Energy Transfer. *New J. Phys.* **2015**, *17* (11), 113052. https://doi.org/10.1088/1367-2630/17/11/113052.

(17) Dung, H. T.; Knöll, L.; Welsch, D. G. Intermolecular Energy Transfer in the Presence of Dispersing and Absorbing Media. *Phys. Rev. A. At. Mol. Opt. Phys.* **2002**, *65* (4), 438131–4381313. https://doi.org/10.1103/PhysRevA.65.043813.

(18) Konrad, A.; Metzger, M.; Kern, A. M.; Brecht, M.; Meixner, A. J. Controlling the Dynamics of Förster Resonance Energy Transfer inside a Tunable Sub-Wavelength Fabry-Pérot-Resonator. *Nanoscale* **2015**, *7* (22), 10204–10209. https://doi.org/10.1039/c5nr02027a.

(19) Rabouw, F. T.; Den Hartog, S. A.; Senden, T.; Meijerink, A. Photonic Effects on the Förster Resonance Energy Transfer Efficiency. *Nat. Commun.* **2014**, *5*, 1–6. https://doi.org/10.1038/ncomms4610.

(20) De Dood, M. J. A.; Knoester, J.; Tip, A.; Polman, A. Förster Transfer and the Local Optical Density of States in Erbium-Doped Silica. *Phys. Rev. B - Condens. Matter Mater. Phys.* **2005**, *71* (11), 1–5. https://doi.org/10.1103/PhysRevB.71.115102.

(21) Blum, C.; Zijlstra, N.; Lagendijk, A.; Wubs, M.; Mosk, A. P.; Subramaniam, V.; Vos, W. L. Nanophotonic Control of the Förster Resonance Energy Transfer Efficiency. *Phys. Rev. Lett.* **2012**, *109* (20), 203601. https://doi.org/10.1103/PhysRevLett.109.203601.

(22) Wubs, M.; Vos, W. L. Förster Resonance Energy Transfer Rate in Any Dielectric Nanophotonic Medium with Weak Dispersion. *New J. Phys.* **2016**, *18* (5). https://doi.org/10.1088/1367-2630/18/5/053037.

(23) Andrew, P.; Barnes, W. L. Science-2004-Andrew-1002-5. *Annu. Rev. Astron. Astrophys* **2004**, *306* (November), 1002–1005.

(24) Nakamura, T.; Fujii, M.; Miura, S.; Inui, M.; Hayashi, S. Enhancement and Suppression of Energy Transfer from Si Nanocrystals to Er Ions through a Control of the Photonic Mode Density. *Phys. Rev. B - Condens. Matter Mater. Phys.* **2006**, *74* (4), 1–6. https://doi.org/10.1103/PhysRevB.74.045302.

(25) Ghenuche, P.; de Torres, J.; Moparthi, S. B.; Grigoriev, V.; Wenger, J. Nanophotonic Enhancement of the Förster Resonance Energy-Transfer Rate with Single Nanoapertures. *Nano Lett.* **2014**, *14* (8), 4707–4714. https://doi.org/10.1021/nl5018145.

(26) Ghenuche, P.; Mivelle, M.; De Torres, J.; Moparthi, S. B.; Rigneault, H.; Van Hulst, N. F.; García-Parajó, M. F.; Wenger, J. Matching Nanoantenna Field Confinement to FRET Distances Enhances Förster Energy Transfer Rates. *Nano Lett.* **2015**, *15* (9), 6193–6201. https://doi.org/10.1021/acs.nanolett.5b02535.

(27) Zhang, X.; Marocico, C. A.; Lunz, M.; Gerard, V. A.; Gun'Ko, Y. K.; Lesnyak, V.; Gaponik, N.; Susha, A. S.; Rogach, A. L.; Bradley, A. L. Wavelength, Concentration, and Distance Dependence of Nonradiative Energy Transfer to a Plane of Gold Nanoparticles. *ACS Nano* **2012**, *6* (10), 9283–9290. https://doi.org/10.1021/nn303756a.

(28) Bidault, S.; Devilez, A.; Ghenuche, P.; Stout, B.; Bonod, N.; Wenger, J. Competition between Förster Resonance Energy Transfer and Donor Photodynamics in Plasmonic Dimer Nanoantennas. *ACS Photonics* **2016**, *3* (5), 895–903. https://doi.org/10.1021/acsphotonics.6b00148.

(29) Ren, J.; Wu, T.; Yang, B.; Zhang, X. Simultaneously Giant Enhancement of Förster Resonance Energy Transfer Rate and Efficiency Based on Plasmonic Excitations. *Phys. Rev. B* **2016**, *94* (12), 1–8. https://doi.org/10.1103/PhysRevB.94.125416.

(30) Zurita-Sánchez, J. R.; Méndez-Villanueva, J. Förster Energy Transfer in the Vicinity of Two Metallic Nanospheres (Dimer). *Plasmonics* **2018**, *13* (3), 873–883. https://doi.org/10.1007/s11468-017-0583-4.

(31) Higgins, L. J.; Marocico, C. A.; Karanikolas, V. D.; Bell, A. P.; Gough, J. J.; Murphy, G. P.; Parbrook, P. J.; Bradley, A. L. Influence of Plasmonic Array Geometry on Energy Transfer from a Quantum Well to a Quantum Dot Layer. *Nanoscale* **2016**, *8* (42), 18170–18179. https://doi.org/10.1039/c6nr05990b.

(32) Schleifenbaum, F.; Kern, A. M.; Konrad, A.; Meixner, A. J. Dynamic Control of Förster Energy Transfer in a Photonic Environment. *Phys. Chem. Chem. Phys.* **2014**, *16* (25), 12812–12817. https://doi.org/10.1039/c4cp01306a.

(33) Russell, K. J.; Liu, T.; Cui, S.; Hu, E. L. Large Spontaneous Emission Enhancement in Plasmonic Nanocavities. **2012**, *6* (July). https://doi.org/10.1038/NPHOTON.2012.112.

(34) Edwards, A. P.; Adawi, A. M. Plasmonic Nanogaps for Broadband and Large Spontaneous Emission Rate Enhancement. *J. Appl. Phys.* **2014**, *115* (5). https://doi.org/10.1063/1.4864018.

(35) Akselrod, G. M.; Argyropoulos, C.; Hoang, T. B.; Ciracì, C.; Fang, C.; Huang, J.; Smith, D. R.; Mikkelsen, M. H. Probing the Mechanisms of Large Purcell Enhancement in Plasmonic Nanoantennas. *Nat. Photonics* **2014**, *8*, 835.

(36) Chikkaraddy, R.; De Nijs, B.; Benz, F.; Barrow, S. J.; Scherman, O. A.; Rosta, E.; Demetriadou, A.; Fox, P.; Hess, O.; Baumberg, J. J. Single-Molecule Strong Coupling at Room Temperature in Plasmonic Nanocavities. *Nature* **2016**, *535* (7610), 127–130. https://doi.org/10.1038/nature17974.

(37) Sykes, M. E.; Stewart, J. W.; Akselrod, G. M.; Kong, X. T.; Wang, Z.; Gosztola, D. J.; Martinson, A. B. F.; Rosenmann, D.; Mikkelsen, M. H.; Govorov, A. O.; Wiederrecht, G. P. Enhanced Generation and Anisotropic Coulomb Scattering of Hot Electrons in an Ultra-Broadband Plasmonic Nanopatch Metasurface. *Nat. Commun.* **2017**, *8* (1). https://doi.org/10.1038/s41467-017-01069-3.

(38) Marshall, A. R. L.; Stokes, J.; Viscomi, F. N.; Proctor, J. E.; Gierschner, J.; Bouillard, J. S. G.; Adawi, A. M. Determining Molecular Orientation: Via Single Molecule SERS in a Plasmonic Nano-Gap. *Nanoscale* **2017**, *9* (44), 17415–17421. https://doi.org/10.1039/c7nr05107g.

(39) Marshall, A. R. L.; Roberts, M.; Gierschner, J.; Bouillard, J.-S. G.; Adawi, A. M. Probing the Molecular Orientation of a Single Conjugated Polymer via Nanogap SERS. *ACS Appl. Polym. Mater.* **2019**, *1* (5), 1175–1180. https://doi.org/10.1021/acsapm.9b00180.

(40) https://www.lumerical.com/tcad-products/fdtd. No Title.

(41) Kristensen, P. T.; Hughes, S. Modes and Mode Volumes of Leaky Optical Cavities and

Plasmonic Nanoresonators. *ACS Photonics* **2014**, *1* (1), 2–10. https://doi.org/10.1021/ph400114e.

(42) Cazé, A.; Pierrat, R.; Carminati, R. Spatial Coherence in Complex Photonic and Plasmonic Systems. *Phys. Rev. Lett.* **2013**, *110* (6), 63903. https://doi.org/10.1103/PhysRevLett.110.063903.

(43) Huang, Y. G.; Chen, G.; Jin, C. J.; Liu, W. M.; Wang, X. H. Dipole-Dipole Interaction in a Photonic Crystal Nanocavity. *Phys. Rev. A - At. Mol. Opt. Phys.* **2012**, *85* (5), 1–7. https://doi.org/10.1103/PhysRevA.85.053827.

(44) Johnson, P. B.; Christy, R. W. Optical Constants of the Noble Metals. *Phys. Rev. B* **1972**, *6* (12), 4370–4379. https://doi.org/10.1103/PhysRevB.6.4370.

(45) Karanikolas, V.; Marocico, C. A.; Bradley, A. L. Spontaneous Emission and Energy Transfer Rates near a Coated Metallic Cylinder. *Phys. Rev. A - At. Mol. Opt. Phys.* **2014**, *89* (6), 1–13. https://doi.org/10.1103/PhysRevA.89.063817.

(46) Yu, Y.-C.; Liu, J.-M.; Jin, C.-J.; Wang, X.-H. Plasmon-Mediated Resonance Energy Transfer by Metallic Nanorods. *Nanoscale Res. Lett.* **2013**, *8* (1), 209. https://doi.org/10.1186/1556-276X-8-209.

(47) Nordlander, P.; Prodan, E. Plasmon Hybridization in Nanoparticles near Metallic Surfaces. *Nano Lett.* **2004**, *4* (11), 2209–2213. https://doi.org/10.1021/nl0486160.

Figures

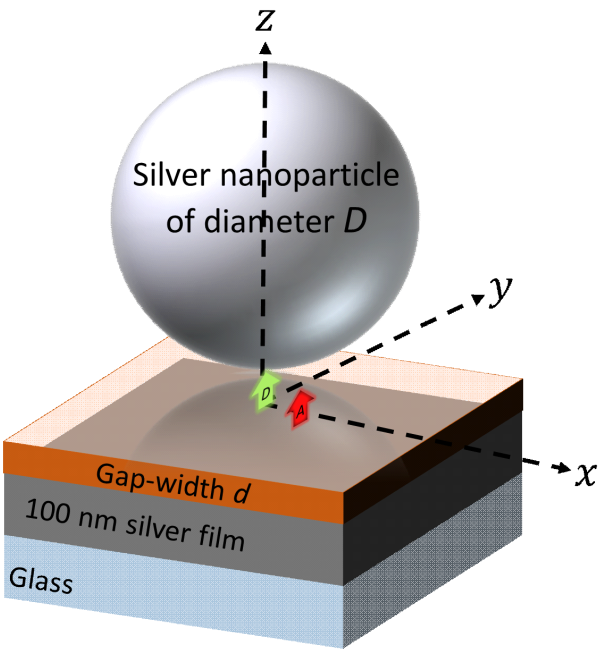

Figure 1. Schematic representation of the plasmonic nanogaps investigated in this work.

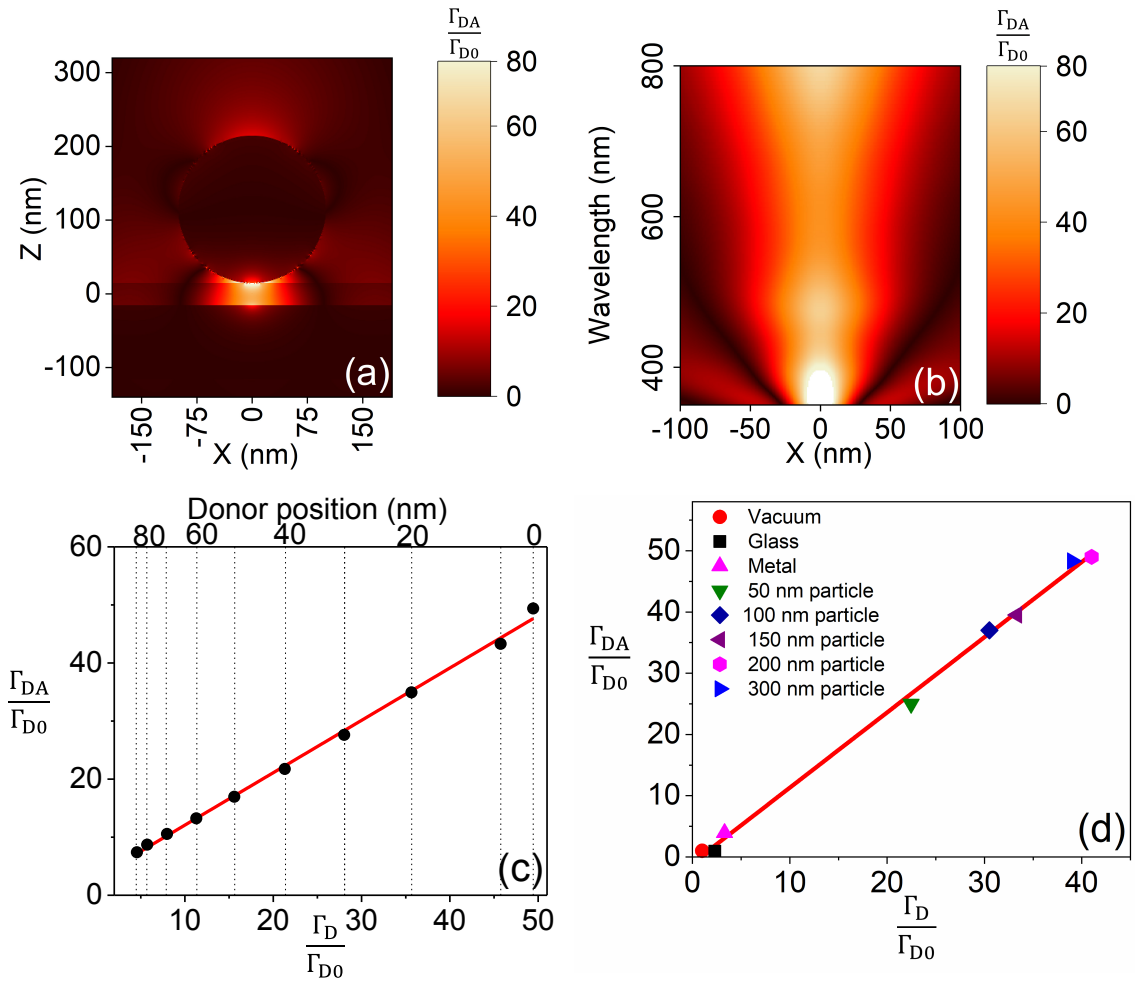

Figure 2. Calculated normalised Förster energy transfer rate enhancement for a 30 nm nanogap formed between a silver particle of diameter and a 100 nm extend silver. (a) As a function of the acceptor position in the x-z plane at and . (b) As a function of the acceptor positon along the line and the donor wavelength . (c) As a function of the donor position along the line with and . (d) As a function of donor decay rate enhancement (or LDOS).

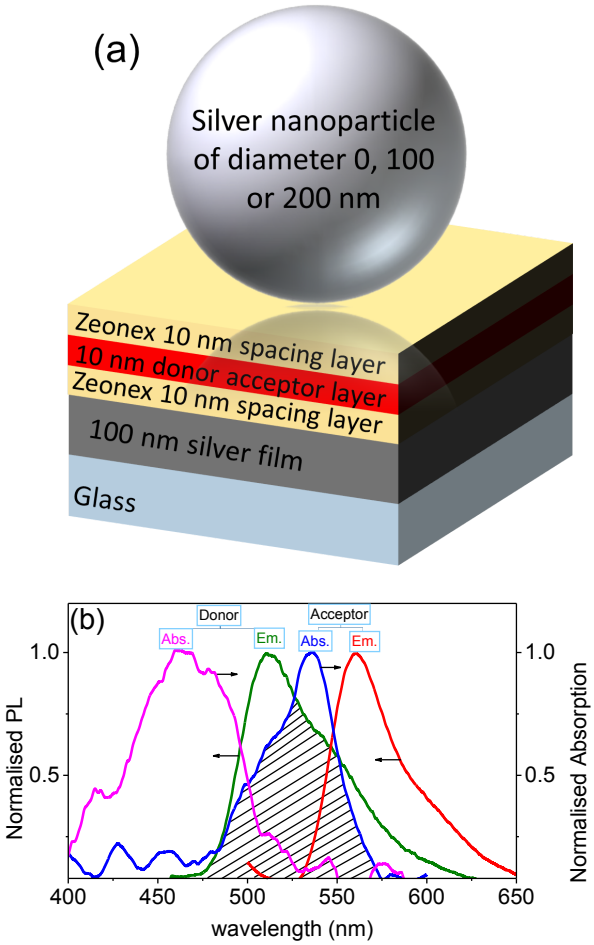

Figure 3. (a) Schematic of the experimentally fabricated silver plasmonic nanogaps. (b) Normalised absorption and emission spectra of the experimentally used donor (Uranin dye)-acceptor (Rhodamine 6G) pair. The shaded area marks the spectral overlap between the absorption spectrum of the donor and the emission spectrum of the acceptor.

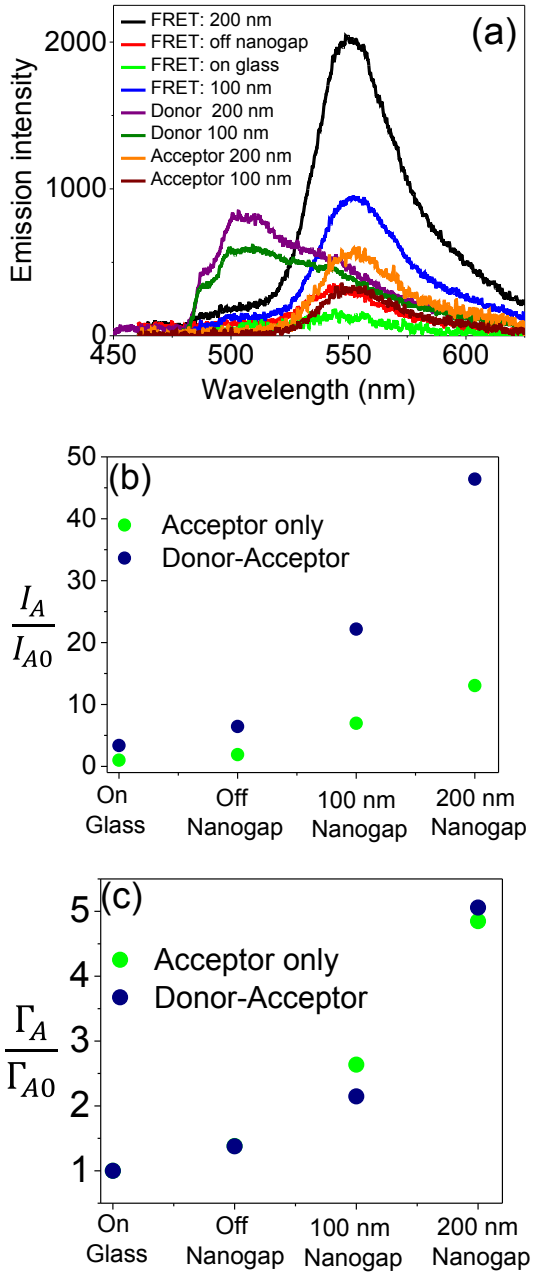

Figure 4. (a) Fluorescence spectra of the donor-acceptor pair measured from 30 nm plasmonic nanogaps with silver particles of diameter, 0 nm, 100 nm and 200 nm. For comparison, data are shown for donor only in 30 nm nanogap with a 100 nm silver particle, acceptor only in a 30 nm nanogap with a 200 nm silver particle and donor-acceptor pair on glass. (b) Measured enhancement in the acceptor emission intensity with and without donor for different nanogaps. (c) Measured enhancement in the acceptor decay with and without donor for different nanogaps.

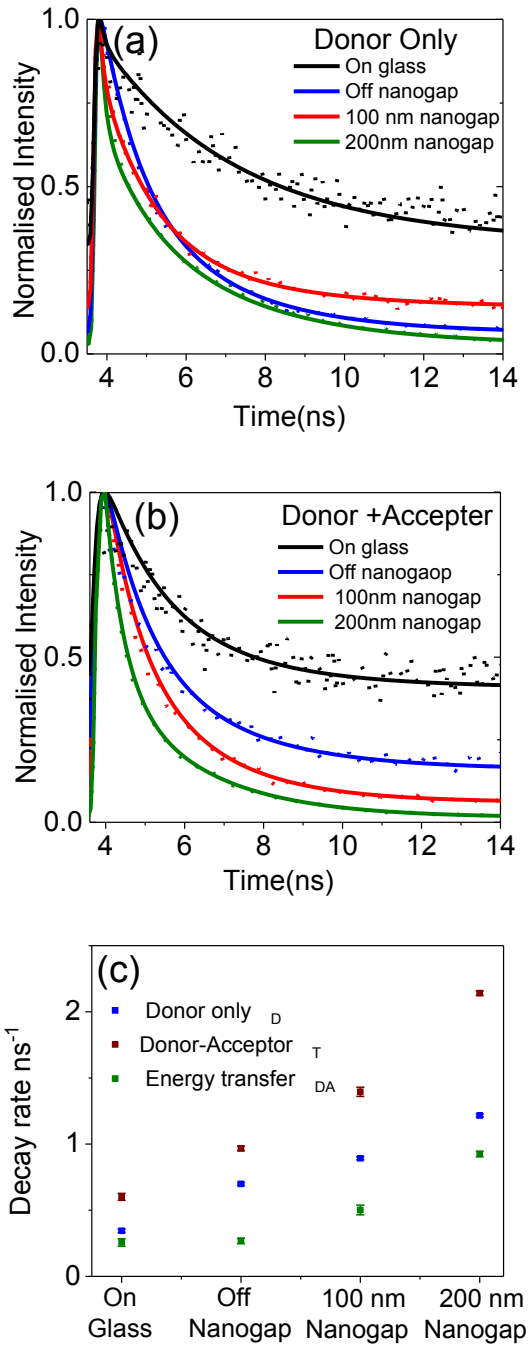

Figure 5. Fluorescence decay curves of donor only (a) and donor-acceptor pair (b) measured from 30 nm plasmonic nanogaps with silver particles of diameter, 0 nm, 100 nm and 200 nm and on glass. (c) Donor only decay rate , total decay rate of the donor in the presence of the acceptor and energy transfer rate from 30 nm plasmonic nanogaps with silver particles of diameter, 0 nm, 100 nm and 200 nm and on glass.

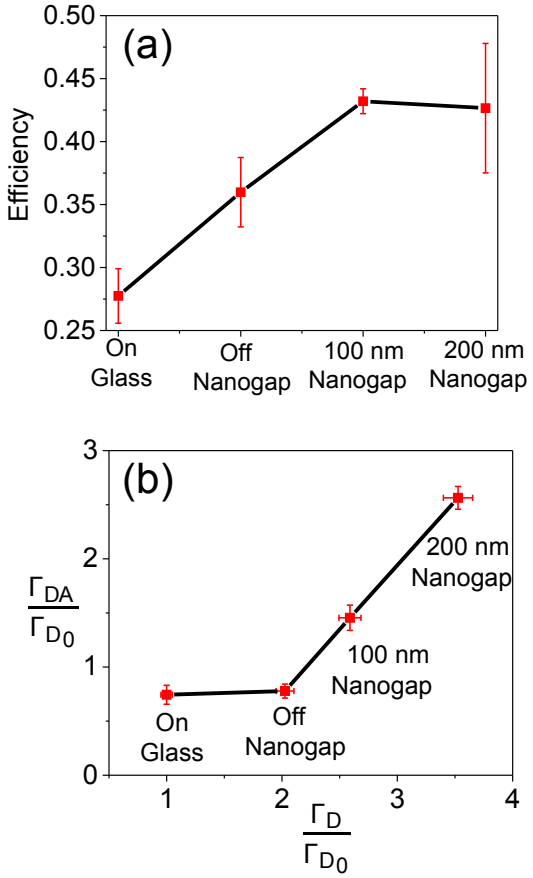

Figure 6. Energy transfer efficiency (a) and normalised Förster energy transfer rate enhancement for a 30 nm nanogap with silver particles of diameter, 0 nm, 100 nm and 200 nm and on glass.